Stabilizing the Zigzag Edge: Graphene Nanoribbons with Sterically Constrained Terminations

Cheng-Ing Chia[1,2] and Vincent H. Crespi[1,2,3]

[1]*Department of Physics, Pennsylvania State University, 104 Davey Lab, University Park, Pennsylvania 16802, USA*
[2]*The Materials Research Institute, Pennsylvania State University, N-317 Millennium Science Complex, University Park, Pennsylvania 16802, USA*
[3]*Department of Materials Science and Engineering, Pennsylvania State University, 121 Steidle Building, University Park, Pennsylvania 16802, USA*

(Received 23 July 2011; revised manuscript received 10 March 2012; published 16 August 2012)

The zigzag edge of a graphene nanoribbon is predicted to support a spin-polarized edge state. However, this edge state only survives under a pure sp^2 termination, and it is difficult to produce thermodynamic conditions that favor a pure sp^2 termination of a graphene edge, since the edge carbons generally prefer to bond to two hydrogen atoms in sp^3 hybridization, rather than one hydrogen, as sp^2. We describe how to use the steric effects of large, bulky ligands to modify the thermodynamics of edge termination and favor the sp^2 edge during, e.g., chemical vapor deposition. *Ab initio* calculations demonstrate that these alternative terminations can support robust edge states across a broad range of thermodynamic conditions. This method of exploiting steric crowding effects along the one-dimensional edge of a two-dimensional system may be a general way to control edge reconstructions across a range of emerging single-layer systems.

DOI: 10.1103/PhysRevLett.109.076802 PACS numbers: 73.22.Pr, 68.43.Fg, 71.15.Mb, 73.20.At

The unusual electronic properties of graphene, including ultrahigh electron mobility and Dirac fermions, have ignited intense research interest directed towards both fundamental physics [1–3] and potential device applications [4,5]. Graphene nanoribbons are particularly intriguing since they both provide a means to generate quantum-confinement gaps [6,7] and spin-polarized edge states on the zigzag edge [8,9], possibly including voltage-tunable half metals [10]. Such ribbons could be fabricated either by lithography [11,12], chemical vapor deposition [13,14], sonochemical [15,16] or chemical cutting of graphene sheets [17,18], or unzipping of nanotubes [19,20]. Different theoretical studies including tight binding [21–24], mean-field theory [25–29], renormalization group [30], continuum models [31], quantum Monte Carlo calculations [32,33], and density functional theory [34–37] have found a spin-polarized edge state on the zigzag edges of graphene nanoribbons. However, the edge state supported by the zigzag edge requires a specific edge termination: a single, single-bonded ligand attached to each edge carbon to retain the sp^2 bond geometry and liberate a π electron to populate the edge state. In contrast, a pair of single-bonded ligands on each edge carbon would generate local sp^3 coordination at the edge, and this termination does not support an edge state. Unfortunately, a careful computational study of hydrogen-terminated ribbons demonstrated that the less interesting sp^3 termination (as depicted in Fig. 1) is thermodynamically favorable across a wide range of conditions [38,39]; the sp^2 edge geometry is favored only at extremely low hydrogen partial pressures.

Here, we demonstrate that steric effects induced by a careful choice of capping ligand can reverse this thermodynamic preference and make the desirable sp^2 termination thermodynamically favored across a broad range of conditions. To understand the geometrical crowding effects at a zigzag edge, consider idealized spherical ligands attached to a zigzag edge, each at a typical single-bond distance

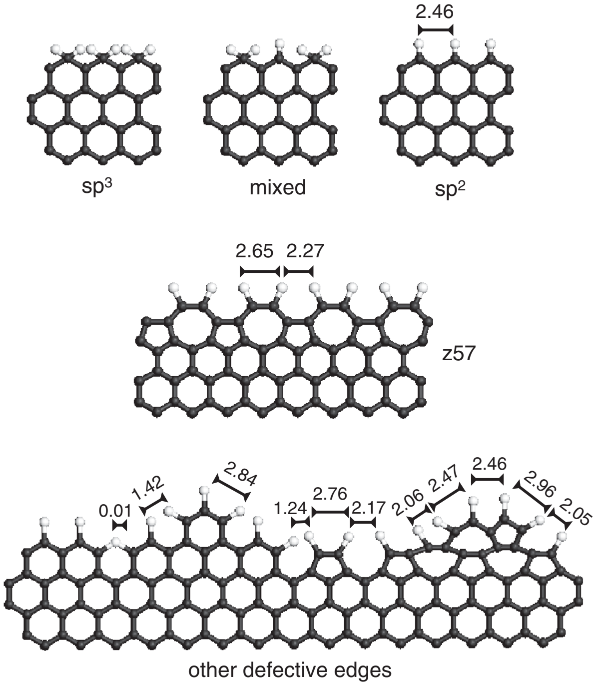

FIG. 1. Top: Three possible edge terminations for a zigzag graphene nanoribbon: pure sp^2 (Z_1), pure sp^3 (Z_2), and a mixed state (Z_{21}) with alternating configurations. Center: A reconstructed zigzag edge with alternating pentagon and heptagon rings. Bottom: Other kinds of defective zigzag edges. All distances are in units of angstroms.

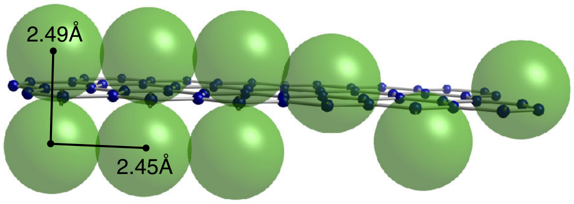

FIG. 2 (color online). A schematic diagram showing the distances between terminating groups on neighboring edge atoms or the same edge atom for an sp^3-terminated zigzag graphene edge. The right side shows the stagger induced on an sp^2 edge for sufficiently large capping ligands.

(1.5 Å) from the edge carbon atom. As a thought experiment, allow these ligands to expand in radius. Figure 2 depicts the resulting geometries for both sp^2 and sp^3 terminations. Surprisingly, the ligands on neighboring edge carbons are actually closer to each other (2.45 Å) than are the two ligands both attached to the same carbon atom (2.49 Å). Hence, capping ligands will collide first between neighboring edge carbons, and only later will ligands at the same carbon collide. However, the more roomy geometry of sp^2 termination allows for a mode of elastic accommodation that is unavailable to the sp^3 case: the ligands can stagger up and down, out of each others' way, as depicted on the right side of Fig. 2. We seek capping ligands sufficiently large that crowding between ligands on neighboring edge carbons forces stagger and, hence, suppresses the sp^3 termination. More generally, the strategy of exploiting geometrical crowding effects along the one-dimensional edge of a two-dimensional sheet may provide a general means of controlling edge reconstructions across broad classes of single-layer or few-layer systems.

Highly symmetric termination groups are particularly attractive, since they provide the minimal number of internal degrees of freedom to accommodate elastic deformation without stagger. We have considered two such ligands: methyl [$-\mathrm{CH_3}$] and the larger tertiary-butyl [$-\mathrm{C(CH_3)_3}$]. Highly substituted molecules with similar ligands (decamethylanthracene, dodecamethyltetracene) are known [40–42]. If these terminating groups are to be introduced during the synthesis of graphene (e.g., during chemical vapor deposition at elevated temperatures), then the primary carbon feedstock that builds the graphene should be a more active hydrocarbon species (such as triple-bonded acetylene), and the reaction conditions (i.e., temperature, pressure, carrier gas, precursor concentrations, etc.) should be tuned so that the precursors to the desired terminating groups (which are more saturated and, hence, likely to be more stable than acetylene) do not also decompose, and undesirable side reactions are suppressed. In the elevated temperature regime characteristic of, e.g., chemical vapor deposition, an energetic comparison of various possible edge terminations can provide useful guidance as to the most favored edge geometry.

We performed plane-wave density functional calculations using the VIENNA *ab initio* simulation package using projected augmented waves [43] with the Perdew-Burke-Ernzerhof [44] variant of the generalized gradient approximation, an energy cutoff of 400 eV, and a $13 \times 1 \times 1$ Monkhorst-Pack grid [45]. All structures are simulated in periodic supercells within a slab geometry, structurally relaxed with total energies converged to 10 meV. The c axis distance between two nanoribbons is 30 Å and the center-to-center in-plane distance between two ribbons is 40 Å independent of ribbon width, which is varied from $N = 4$ to $N = 12$ following the standard $(N, 0)$ notation for zigzag nanoribbon structures. Since the system must be able to accommodate a staggered, geometrically crowded ligand geometry, the unit cell along the ribbon axis is at least double the pristine graphenic cell length. Non-spin-polarized, ferromagnetic, and antiferromagnetic interedge spin configurations are considered, using the non-spin-polarized case for structural relaxation (magnetic energies have little effect on the structural relaxation). Following the notation from the work of T. Wassmann *et al.* [38,39], we denote a zigzag edge with $n_i = 1, 2$ terminating groups on the ith site as $Z_{n_1 n_2 \ldots n_x}$, as depicted in Fig. 1.

To compare the stabilities of sp^3, sp^2, and mixed (alternating sp^3 and sp^2) edge terminations, one requires a reference chemical potential for the capping ligand. For the methyl ligand, a natural reference choice is the methyl dimer, i.e., ethane. We studied the nanoribbons with different edge terminations in periodic supercells, including the alternating pentagon-heptagon reconstruction shown in Fig. 1 [46,47], which we call ZZ_{57}. At the lowest ethane chemical potentials the system prefers the desired pure-sp^2 Z_1 termination, transitioning to more complex Z_{2111}, Z_{221} and Z_{2221} termination patterns at chemical potentials of 0.2, 0.9, and 1.2 eV, respectively. The various sp^2 and/or sp^3 terminations of the ZZ_{57} reconstruction are not favored and do not appear on the phase diagram.

The unfavorability of the ZZ_{57} reconstruction reflects its less uniform edge geometry: whereas the unreconstructed pure-hexagon edge has a uniform spacing between ligand attachment points, the ZZ_{57} edge has alternating long and short spacings, as shown in Fig. 1. In systems with bulky ligands that are dominated by repulsive steric interactions, the shortest such spacing dominates the energetics and thus reduces the stability of the reconstruction relative to the ideal hexagonal edge. A similar geometrical effect should apply to other defective edge structures, such as those shown at the bottom of Fig. 1, under steric constraint: in each of these cases, the defect contains a subset of short interligand spacings which will raise the relative energy of that defect. This general principle suggests that introduction of tightly bound, bulky edge ligands might be a useful strategy to suppress defect formation on the edges of atomically thin two-dimensional systems, thereby favoring the production of ideal, defect-free edges.

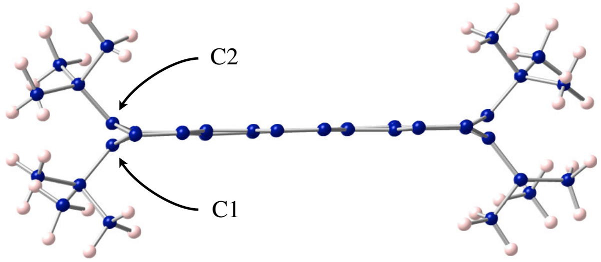

FIG. 3 (color online). Side view of a tert-butyl terminated carbon nanoribbon with $N = 6$. The edge carbon atoms of the nanoribbon (labeled C1 and C2) stagger alternately up and down to accommodate the bulky tert-butyl capping ligands.

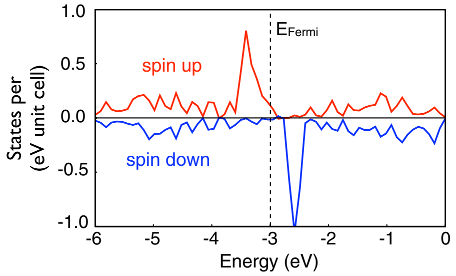

FIG. 4 (color online). Calculated spin-polarized density of states projected onto the carbon atoms along one edge of an antiferromagnetic, tert-butyl terminated $N = 12$ nanoribbon.

As discussed above, methyl ligands successfully stabilize the desired Z_1 pure-sp^2 termination at low ligand chemical potentials. Replacing each hydrogen atom in $-\mathrm{CH_3}$ by a methyl group produces $-\mathrm{C(CH_{33})}$, tertiary-butyl, a bulkier ligand which may favor Z_1 across a broader range of thermodynamic conditions. The tert-butyl radical is so large that all sp_3-containing terminations are highly unfavorable energetically compared to the pure-sp^2 Z_1 configuration. In addition, this very bulky ligand may provide kinetic stability through steric protection of the zigzag bond.

As expected, the terminating ligands in the relaxed structure stagger alternately up and down, as shown in Fig. 3. This buckling is an inescapable consequence of the steric crowding geometry of the zigzag edge, since ligands at neighboring edge carbons are closer to each other than would be two ligands on the same carbon (in fact, initial displacements of the tert-butyl groups away from planarity are required to ensure a well-behaved structural relaxation). But does this stagger come at too high a price? I.e., does the spin-polarized edge state survive the geometrical deformations necessary to thermodynamically stabilize it?

Energetically, the antiferromagnetic state of the tert-butyl-terminated ribbon is the most stable of the three options considered (within the limits of density functional theory), just as it is for a standard hydrogen-terminated sp^2 zigzag nanoribbon: it is 0.05 eV per unit cell lower in energy than the ferromagnetic state and 0.15 eV lower than the non-spin-polarized state for $N = 4$ (with similar energetic ordering for wider ribbons, albeit with smaller absolute energy differences due to the weaker edge-to-edge interaction across the wider ribbons). The density of states projected to one edge in the antiferromagnetic state (see Fig. 4) has a pronounced peak for one spin channel below the Fermi energy with the other channel appearing above E_F, as expected. Although the accuracy of density functional theory in discerning the energetic order of magnetically ordered states is limited, this does not affect our primary conclusions on the thermodynamic stability of the zigzag edge, which occurs on a much higher energy scale.

A comparison of the detailed bandstructures for the three magnetic states with those of the standard hydrogen-terminated versions, as shown in Fig. 5, supports the view that the spin-polarized edge state survives the staggering deformation. The bands near the Fermi energy are similar in both cases, whether the partly flat nonmagnetic band, the ferromagnetic band crossing, or the weakly gapped antiferromagnetic state. The main physical effect of the staggering in the tert-butyl terminated nanoribbon is a slight increase in the dispersion of the edge state(s) and a slight band splitting arising most likely from the doubled unit cell. The small increase in band dispersion may be due to a lowering of the on-site energy on the tilted edge carbons [48] due to the higher electronegativity of tert-butyl compared to a simple hydrogen termination.

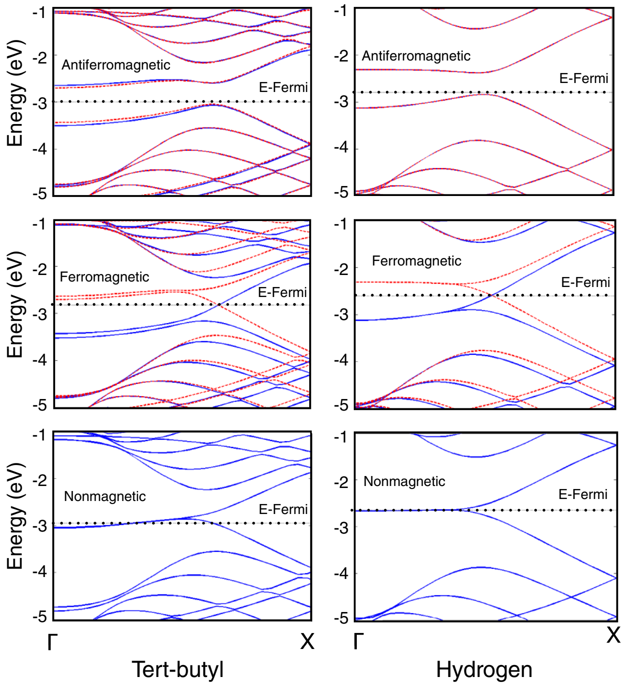

FIG. 5 (color online). The band structures of a tert-butyl terminated $N = 12$ zigzag nanoribbon in different magnetic states (left), as compared to a similar nanoribbon terminated with simple hydrogen atoms (right). Blue solid lines and red dashed lines represent opposite spin states.

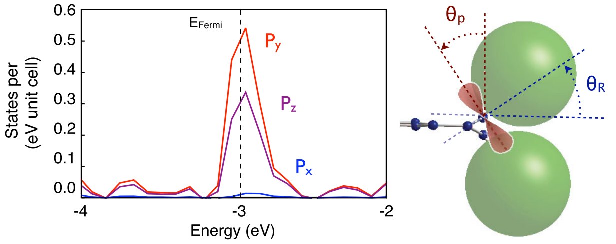

FIG. 6 (color online). Left: Projected density of the state of the p orbital on single side edge carbon atom ($N = 12$) for the non-spin-polarized calculation. Right: Θ_R measures the tilt angle of the edge carbon atom in terms of the location of the attached tert-butyl group. Θ_p measures this angle in terms of the rotation of the atom's π orbital.

Analysis of the site-projected density of states on the edge carbon atoms further supports the existence of an edge state for these sterically constrained nanoribbon terminations. Taking the non-spin-polarized case for simplicity, the edge carbon state at the Fermi level projects onto both $2p_y$ and $2p_z$ orbitals, as shown in Fig. 6, rather than just onto $2p_z$ as would be the case for a standard flat nanoribbon (z is perpendicular to the plane of the ribbon, and y is transverse to the ribbon axis). This superposition arises from the stagger. We can compare the tilt angle defined in terms of the projected densities of states, $\Theta_p = \tan^{-1}\left(D_y/D_z\right)$, to the tilt angle defined in real space, $\Theta_R = \tan^{-1}\frac{\Delta_z}{\Delta_y}$ for Δ_y, Δ_z the displacements from the center of the tert-butyl ligand to the edge carbon atom. Θ_R and Θ_p differ by less than 1° for an $N = 12$ ribbon and are similarly close for other widths. Hence, the graphene edge state retains the expected π character, just tilted due to the sterically-induced stagger.

For reasons of computational tractability, the calculations described above neglect the substrate that is typically present below nonsuspended graphene samples, but this simplification should not alter our main conclusions. For example, angstrom-scale surface roughness would provide some leeway for bulky ligands, as would minor infiltration of solvents underneath the edges of a flake (particularly since the bending energetics of graphene are second order in displacement while the attachment energetics of tightly bound edge ligands are effectively zeroth order). Most importantly, the fact that a substrate acts as a further steric constraint works to the general advantage of the mechanism that we propose: the less overall space available, the more highly favored will be the sp^2-coordinate terminations for bulky ligands. Of course, the specific ligands required may require some fine tuning in an actual experiment.

In conclusion, under normal conditions the edge atoms on a graphene nanoribbon tend to be fully saturated with, e.g., hydrogen to form sp^3 terminations that destroy the magnetic edge state. We have identified a technique to exploit steric crowding to stabilize the sp^2 termination that is needed to generate an electronic graphene edge state. When the size of the terminating group is sufficiently large, these ligands must stagger alternately up and down to get out of each other's way, an accommodation that is not available to the more crowded sp^3 termination. Although we analyzed the case of methyl and tert-butyl in detail, this technique is general to any terminating group of appropriate size and shape and to any graphene edge orientation. By careful tuning of ligand size and shape, it may also be possible to selectively stabilize mixed sp^2 and sp^3 edge structures with unique, tunable properties. Treatments beyond density functional theory could then reveal additional effects due to electron-electron correlation in this low-bandwidth edge-localized state.

We are grateful to Ning Shen and Jorge Sofo for discussions on edge state band dispersion. We acknowledge DMR-0707332 for support in the initial stages of the work and DMR-0820404 and U.S. Army Research Office MURI Grant No. W911NF-11-1-0362 for support in the later stages.

[1] K. S. Novoselov, A. K. Geim, S. V. Morozov, D. Jiang, Y. Zhang, S. V. Dubonos, I. V. Grigorieva, and A. A. Firsov, Science **306**, 666 (2004).

[2] K. S. Novoselov, A. K. Geim, S. V. Morozov, D. Jiang, Y. Zhang, S. V. Dubonos, I. V. Grigorieva, and A. A. Firsov, Nature (London) **438**, 197 (2005).

[3] Y. Zhang, Y.-W. Tan, H. L. Stormer, and P. Kim, Nature (London) **438**, 201 (2005).

[4] A. K. Geim and K. S. Novoselov, Nature Mater. **6**, 183 (2007).

[5] J. Yan, Y. Zhang, P. Kim, and A. Pinczuk, Phys. Rev. Lett. **98**, 166802 (2007).

[6] K. Nakada, M. Fujita, G. Dresselhaus, and M. S. Dresselhaus, Phys. Rev. B **54**, 17954 (1996).

[7] M. Y. Han, B. Ozyilmaz, Y. Zhang, and P. Kim, Phys. Rev. Lett. **98**, 206805 (2007).

[8] C. O. Girit, J. C. Meyer, R. Erni, M. D. Rossell, C. Kisielowski, L. Yang, C.-H. Park, M. F. Crommie, M. L. Cohen, S. G. Louie, and A. Zettl, Science **323**, 1705 (2009).

[9] O. V. Yazyev and M. I. Katsnelson, Phys. Rev. Lett. **100**, 047209 (2008).

[10] Y.-W. Son, M. L. Cohen, and S. G. Louie, Nature (London) **444**, 347 (2006).

[11] M. Y. Han, B. Ozyilmaz, Y. Zhang, and P. Kim, Phys. Rev. Lett. **98**, 206805 (2007).

[12] Z. Chen, Y.-M. Lin, M. J. Rooks, and P. Avouris, Physica (Amsterdam) **40E**, 228 (2007).

[13] X. Jia, M. Hofmann, V. Meunier, B. G. Sumpter, J. Campos-Delgado, J. M. Romo-Herrera, H. Son, Y.-P. Hsieh, A. Reina, J. Kong, M. Terrones, and M. S. Dresselhaus, Science **323**, 1701 (2009).

[14] J. Campos-Delgado, J. M. Romo-Herrera, X. Jia, D. A. Cullen, H. Muramatsu, Y. A. Kin, T. Hayashi, Z. Ren, D. J. Smith, Y. Okuno, T. Ohba, H. Kanoh, K. Kaneko,

M. Endo, H. Terrones, M. S. Dresselhaus, and M. Terrones, Nano Lett. **8**, 2773 (2008).
[15] X. Li, X. Wang, L. Zhang, S. Lee, and H. Dai, Science **319**, 1229 (2008).
[16] X. Wang, Y. Ouyang, X. Li, H. Wang, J. Guo, and H. Dai, Phys. Rev. Lett. **100**, 206803 (2008).
[17] S. S. Datta, D. R. Strachan, S. M. Chamis, and A. T. C. Johnson, Nano Lett. **8**, 1912 (2008).
[18] L. C. Campos, V. R. Manfrinato, J. D. Sanchez-Yamagishi, J. Kong, and P. Jarillo-Herrero, Nano Lett. **9**, 2600 (2009).
[19] D. V. Kosynkin, A. L. Higginbotham, A. Sinitskii, J. R. Lomeda, A. Dimiev, B. K. Price, and J. M. Tour, Nature (London) **458**, 872 (2009).
[20] L. Jiao, L. Zhang, X. Wang, G. Diankov, and H. Dai, Nature (London) **458**, 877 (2009).
[21] K. Wakabayashi, M. Fujita, H. Ajiki, and M. Sigrist, Phys. Rev. B **59**, 8271 (1999).
[22] N. M. R. Peres, A. H. C. Neto, and F. Guinea, Phys. Rev. B **73**, 195411 (2006).
[23] N. M. R. Peres, F. Guinea, and A. H. C. Neto, Phys. Rev. B **73**, 125411 (2006).
[24] M. A. H. Vozmediano, M. P. Lopez-Sancho, T. Stauber, and F. Guinea, Phys. Rev. B **72**, 155121 (2005).
[25] M. Fujita, K. Wakabayashi, K. Nakada, and K. Kusakabe, J. Phys. Soc. Jpn. **65**, 1920 (1996).
[26] J. Fernandez-Rossier and J. J. Palacios, Phys. Rev. Lett. **99**, 177204 (2007).
[27] S. Bhowmick and V. B. Shenoy, J. Chem. Phys. **128**, 244717 (2008).
[28] J. J. Palacios, J. Fernandez-Rossier, and L. Brey, Phys. Rev. B **77**, 195428 (2008).
[29] J. Viana-Gomes, V. M. Pereira, and N. M. R. Peres, Phys. Rev. B **80**, 245436 (2009).
[30] T. Hikihara, X. Hu, H.-H. Lin, and C. Y. Mou, Phys. Rev. B **68**, 035432 (2003).
[31] J. Jung, T. Pereg-Barnea, and A. H. MacDonald, Phys. Rev. Lett. **102**, 227205 (2009).
[32] H. Feldner, Z. Y. Meng, A. Honecker, D. Cabra, S. Wessel, and F. F. Assaad, Phys. Rev. B **81**, 115416 (2010).
[33] H. Feldner, Z. Y. Meng, T. C. Lang, F. F. Assaad, S. Wessel, and A. Honecker, Phys. Rev. Lett. **106**, 226401 (2011).
[34] Y.-W. Son, M. L. Cohen, and S. G. Louie, Phys. Rev. Lett. **97**, 216803 (2006).
[35] L. Yang, C.-H. Park, Y.-W. Son, M. L. Cohen, and S. G. Louie, Phys. Rev. Lett. **99**, 186801 (2007).
[36] K. Kusakabe and M. Maruyama, Phys. Rev. B **67**, 092406 (2003).
[37] L. Pisani, J. A. Chan, B. Montanari, and N. M. Harrison, Phys. Rev. B **75**, 064418 (2007).
[38] T. Wassmann, A. P. Seitsonen, A. M. Saitta, M. Lazzeri, and F. Mauri, Phys. Rev. Lett. **101**, 096402 (2008).
[39] A. P. Seitsonen, A. M. Saitta, T. Wassmann, M. Lazzeri, and F. Mauri, Phys. Rev. B **82**, 115425 (2010).
[40] R. A. Pascal, Jr., Chem. Rev. **106**, 4809 (2006).
[41] A. Sy and H. Hart, J. Org. Chem. **44**, 7 (1979).
[42] H. Hart and S. Shamouilian, J. Org. Chem. **46**, 4874 (1981).
[43] G. Kresse and D. Joubert, Phys. Rev. B **59**, 1758 (1999).
[44] J. P. Perdew, K. Burke, and M. Ernzerhof, Phys. Rev. Lett. **77**, 3865 (1996).
[45] H. J. Monkhorst and J. D. Pack, Phys. Rev. B **13**, 5188 (1976).
[46] P. Koskinen, S. Malola, and H. Hakkinen, Phys. Rev. Lett. **101**, 115502 (2008).
[47] S. M.-M. Dubois, A. Lopez-Bezanilla, A. Cresti, F. Triozon, B. Biel, J.-C. Charlier, and S. Roche, ACS Nano **4**, 1971 (2010).
[48] N. Shen and J. O. Sofo, Phys. Rev. B **83**, 245424 (2011).